Electronic Supplementary Information

Robust Pt nanozyme for visual isoniazid determination in commercial tablets and biosamples

Lili Ai[a,+], Qi Zhang[a,+], Chenwang Zhang[a,+], Zhi Xia[b,*], Xiaoxu Cao[c,*], Yizhou Xu[d], Phouphien Keoingthong[e], Shengkai Li[a,*]

[a] Key Laboratory of Endemic and Ethnic Diseases, Ministry of Education, Key Laboratory of Medical Molecular Biology of Guizhou Province, Center for Tissue Engineering and Stem Cell Research, Key Laboratory of Functional Nucleic Acids-Based Biopharmaceutical Research, School of Basic Medical Sciences, Guizhou Medical University, Guiyang 550025, China

[b] College of Chemistry and Chemical Engineering, Guizhou University of Engineering Science, Bijie 551700, China

[c] Molecular Science and Biomedicine Laboratory (MBL), State Key Laboratory of Chemo/Bio–Sensing and Chemometrics, College of Chemistry and Chemical Engineering, Aptamer Engineering Center of Hunan Province, Hunan Provincial Key Laboratory of Biomacromolecular Chemical Biology, Hunan University, Changsha 410082, China

[d] Department of Infectious Diseases, The First Hospital of Changsha, Changsha 410000, China

[e] Department of Environmental Sciences, Faculty of Environmental Sciences, National University of Laos, 13th Road, Dongdok, Vientiane 01000, Laos

[*] Corresponding authors

E-mail address: zhix@gues.edu.cn (Z. Xia); cxx1356461013@163.com (X. Cao); lishengkai@gmc.edu.cn (S. Li).

1. Experimental Section

1.1 Reagents and instruments

Reagents: All chemical reagents were obtained from Adamas. Commercial isoniazid (INH) tablet was obtained from the pharmacy in Guiyang, Guizhou. Human urine and serum samples were provided by the Affiliated Hospital of Guizhou Medical University. Ethical statemen: The human serum and urine test was reviewed and approved by Ethical Committee of the Guizhou Medical University (Approval Number: No. (12) 2025). All reagents are of analytical grade and used as received without further purification, and double-distilled H_2O (ddH_2O, resistivity of 18.2 MΩ·cm) was used in all experiments.

Instruments: A JEOL 2010 microscope was used for high-resolution transmission electron microscopic (TEM) characterizations. A X'Pert PRO X-ray diffractometer (XRD) and thermo Scientific K-Alpha X-ray photoelectron spectrometer (XPS) were used for structural performance tests. A Shimadzu UV-2450 spectrophotometer was used for UV-vis absorption spectra measurements. A Bruker EMXplus electron paramagnetic resonance spectroscopy (EPR) was used for EPR spectra measurements. A LC-20AT high performance liquid chromatography (HPLC) was used for the quantification detection of INH. An Optima 5300DV inductively coupled plasma optical emission spectrometry (ICP-OES) was used for the quantification detection of Pt.

1.2 Condition-dependent POD-like activity of the Pt-NZ

TMB was used as the colorimetric substrate to study the pH-, temperature-, and catalyst concentration-dependent peroxidase (POD)–like activity of the Pt-NZ. Absorbance at 652 nm was measured after a 5 min incubation period.

(1) pH–dependent study: The experiments were conducted in 1 mL PBS (20 mM, pH 2.0-7.0), containing 0.5 mM TMB, 1.88 mg/L Pt-NZ and 1 mM H_2O_2 at ~30 ℃.

(2) Temperature–dependent study: The experiments were conducted in 1 mL PBS (20 mM, pH 5.0), containing 0.5 mM TMB, 1.88 mg/L Pt-NZ and 1 mM H_2O_2 at different temperatures (10-50 ℃).

(3) TMB concentration–dependent study: The experiments were conducted in PBS (20 mM, pH 5.0), containing 1.88 mg/L Pt-NZ, 1 mM H_2O_2 and various concentrations of TMB (0.1-0.6 mM) at ~30 ℃.

(4) Catalyst concentration–dependent study: The experiments were conducted in PBS (20 mM, pH 5.0), containing 0.4 mM TMB, 1 mM H_2O_2 and various concentrations of Pt-NZ (0.37-2.59 mg/L) at ~30 ℃.

(5) H_2O_2 concentration–dependent study: The experiments were conducted in PBS (20 mM, pH 5.0), containing 0.4 mM TMB, 1.88 mg/L Pt-NZ and various concentrations of H_2O_2 (0.2-1.2 mM) at ~30 ℃.

1.3 Catalytic kinetic study of the Pt-NZ

The steady–state kinetic assay toward TMB was tested with H_2O_2 concentration fixed at 1 mM in 1 mL PBS (20 mM, pH 5.0), while the assay for H_2O_2 was performed with the TMB concentration fixed at 0.5 mM in 1 mL PBS (20 mM, pH 7.0). The absorbance at 652 nm were measured after a 3 min incubation period. The plots of reaction velocity (v) against substrate concentrations were fitted using nonlinear regression of the Michaelis–Menten equation ($v = V_{max} \times [S] / [S] + K_m$, where v, [*S*] and K_m are the initial velocity, substrate concentration

and the Michaelis constant, respectively). The K_m and maximum reaction rate (V_{max}) were obtained from the Lineweavere-Burk double reciprocal plots.

Catalytic mechanism study of Pt-NZ

(1) Radical scavenge experiments: Quenching experiments utilizing tryptophan (Trp), *p*-benzoquinone (*p*-BQ), and isopropanol (IPA) were conducted in 1 mL PBS buffer (20 mM, pH 5.0) containing 0.4 mM 3, 3', 5, 5'–tetramethylbenzidine (TMB), 1.88 mg/L Pt-NZ, and 0.8 mM H_2O_2. The UV-vis absorption spectra of the reaction mixture were recorded following a 30-min incubation period.

(2) Electron paramagnetic resonance (EPR) spectroscopy measurements: EPR analyses were carried out in PBS buffer (20 mM, pH 7.0) using 5,5-dimethyl-1-pyrroline *N*-oxide (DMPO) as the $^{\bullet}OH$ trapping agent. Spectral data were acquired after 5 min of incubation.

(3) DFT calculations: The Pt (111) system was constructed with a vacuum layer of 18 Å along the z-direction to avoid interactions between periodic images. Subsequently, H, OH, H_2O, and/or H_2O_2 species were introduced onto the surface. All atoms were fully relaxed during the calculations. First-principles calculations based on density functional theory (DFT) were performed using the Cambridge Sequential Total Energy Package (CASTEP)[1]. The electron–electron interactions were described within the generalized gradient approximation (GGA) [2] using the Perdew–Burke–Ernzerhof (PBE) functional with norm-conserving pseudopotentials[3]. A plane-wave energy cutoff of 750 eV and a k-point mesh of 7 × 7 × 1 were employed, both of which were confirmed to ensure convergence. The convergence criteria were set as follows: force tolerance below 0.01 eV/Å, energy tolerance per atom below 5.0×10^{-7} eV, and maximum displacement below 5.0×10^{-4} Å. Additionally, Grimme's DFT-D correction was applied to account for van der Waals interactions in all calculations[4].

The adsorption energy of A (where A = H, OH, H_2O, and/or H_2O_2) group was calculated as[4]: $\Delta E_A = E_{*A} - E_* - E_A$, where E_{*A}, E_* and E_A stand for the total energy of adsorbed system, the energy of the clean Pt(111) surface and the energy of the free adsorbate A in the gas phase.

The Gibbs free energy diagrams were evaluated by the following equation[5, 6]: $\Delta G = \Delta E + \Delta ZPE - T\Delta S$, where ΔE is the energy change obtained from DFT calculations; ΔZPE is the change in zero point energy; T is the temperature in Kelvin (set to 300 K in this study), and ΔS is the change in entropy.

Optimization of the reaction time

Prior to colorimetric quantification, the reaction time for the monitoring system was determined based on the saturation point of TMB oxidation catalyzed by the Pt-NZ under optimal experimental conditions. The time required to achieve near-complete saturation was selected as the standard reaction duration.

1. Results and Discussion

Fig. S1

Figure S1. Images showing PBS + H_2O_2 (Left) and PBS + H_2O_2 + Pt-NZ (Right) after a 5-minute incubation.

The catalase-like activity of the Pt-NZ was evaluated under the specified assay conditions (pH 5.0, 0.8 mM H_2O_2, and 1.85 mg/L Pt-NZ). No detectable generation of O2 bubbles was observed, indicating a negligible catalase-like activity.

Fig. S2

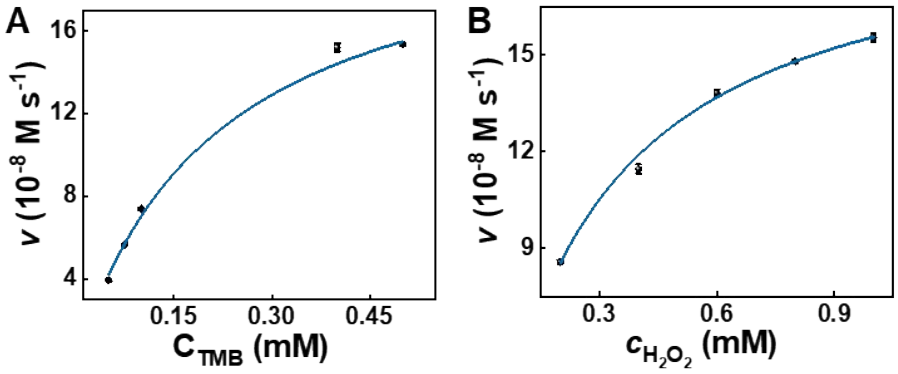

Figure S2. Steady–state kinetic analysis of Pt-NZ activity using (A) TMB and (B) H_2O_2 as substrates.

Fig. S3

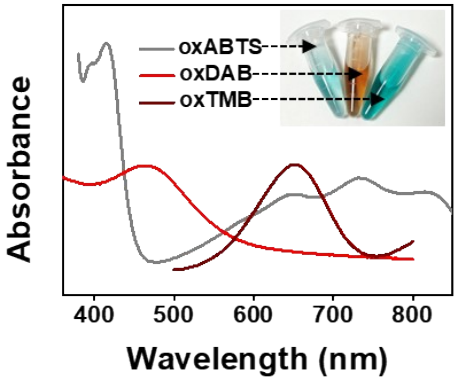

Figure S3. UV-vis absorption spectra and picture of the oxABTS, oxDAB and oxTMB products catalyzed by Pt-NZ. Inset: Pictures of the corresponding chromogenic reactions.

Fig. S4

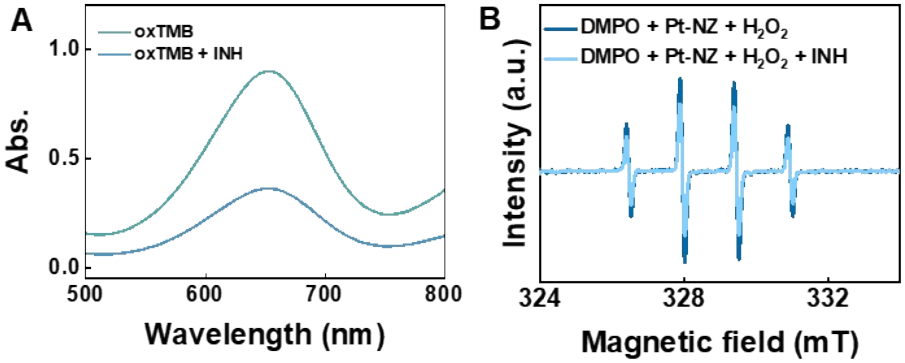

Figure S4. (A) (A) UV-vis absorption spectra of oxTMB (oxTMB was prepared by the Pt-NZ-catalyzed oxidation of TMB in the presence of H_2O_2, with the catalyst subsequently removed by centrifugation) in the presence and absence of INH. (B) EPR spectra of the DMPO-•OH adduct with and without INH. The results above indicated INH could quench •OH and reduce oxTMB.

Fig. S5

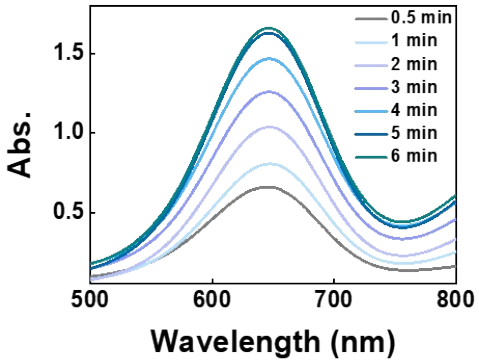

Figure S5. UV-vis absorption spectra showing the time-dependent oxidation of TMB under optimal conditions.

Fig. S6

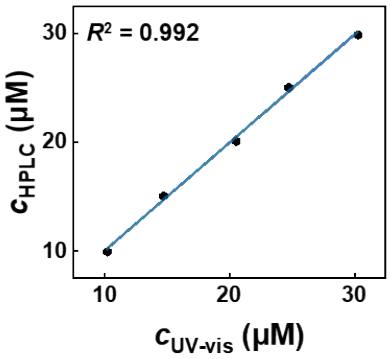

Figure S6. Correlation between the HPLC method and the developed colorimetric method for INH detection in artificial urine samples.

Fig. S7

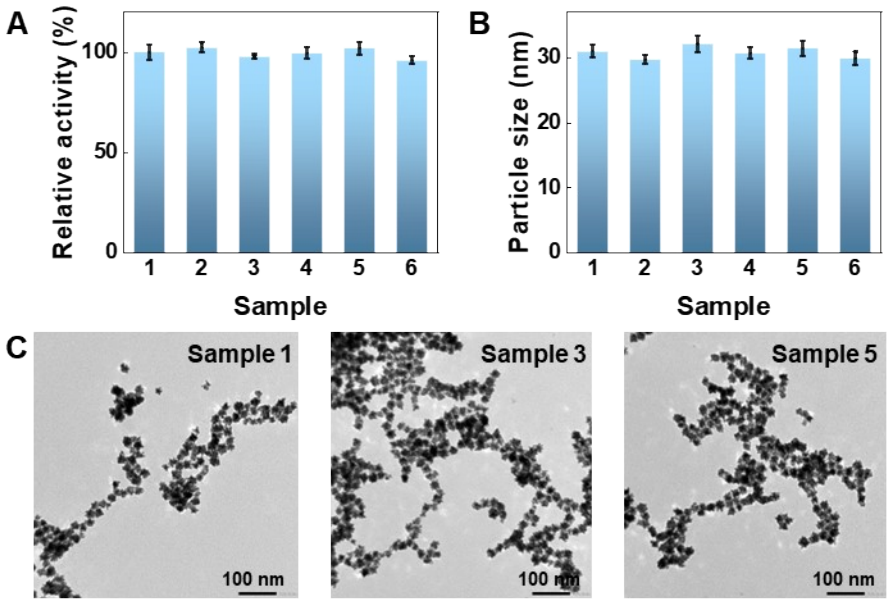

Figure S7. Evaluation of intra- and inter-batch consistency for Pt-NZ. The six Pt-NZ samples were evaluated for (A) relative POD-like activity and (B) hydrodynamic diameter. The samples were prepared over three days (pairs: 1&2, 3&4, 5&6), and all values are reported with respect to sample 1. (C) Corresponding TEM images of select samples (1, 3, and 5).

Fig. S8

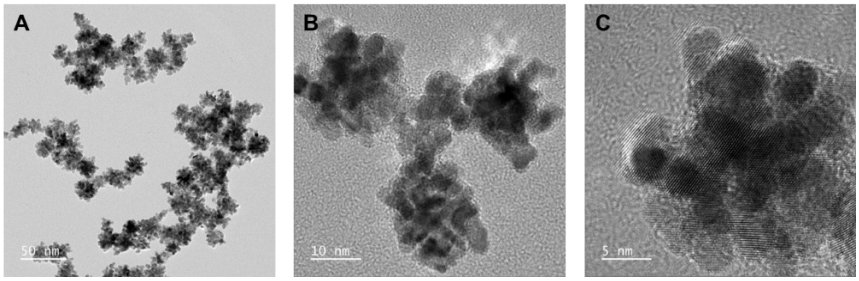

Figure S8. TEM images of the Pt-NZ after the colorimetric INH detection at various magnifications.

Table S1

Table S1. Comparison of dynamic parameters of Pt-NZ with other POD–like Pt-based nanozymes.

Nanozyme	Substrate	K_m (mM)	V_{max} ($\times 10^{-7}$ M s^{-1})	Reference
HRP	TMB	0.434	1.0	[7]
	H_2O_2	3.70	0.871	
RET2-Pt2.9	TMB	0.056	5.82	[8]
	H_2O_2	48	5.68	
ATT-Pt	TMB	0.3026	0.579	[9]
	H_2O_2	1.046	0.926	
Pt_{600}-GLP NCs	TMB	0.22	5.58	[10]
	H_2O_2	0.17	0.504	
BSA-PtNPs	TMB	0.217	1.54	[11]
	H_2O_2	6.84	2.87	
CoPt@G	TMB	2.06	0.751	[12]
	H_2O_2	3.56	8.99	
Pt-NZ	TMB	0.21	2.21	**This work**
	H_2O_2	0.25	1.96	

Table S2

Table S2. Comparative analysis of the INH sensing performance enabled by Pt-NZ and other nanozymes.

Nanozyme	Detection range	LOD	Reference
CuFe–PBA–NC	1–100	0.44	[13]
Mo–MnO_2 NFs	1–40	0.436	[14]
CuO/NiO NTs	1–20	0.4	[15]
PtRuMoCoNi	1.5–50	2.3	[16]
Copper carbonate analog	0–178.6	8.47	[17]
FeCu–NC	0.9–10	0.3	[18]
Py–PD COF	2–100	1.26	[19]
Mn–PBA–DSNB@Au	2–40	0.835	[20]
HS–PtNPs	2.5–250	1.7	[21]
Pt-NZ	5.0–35	1.46	**This work**

Table S3

Table S3. Experimental results from two independent experiments demonstrate the detection of INH in commercial tablets, urine, and serum, all assays conducted with the same batch of Pt-NZ (different from the one in Figure 5).

Experimental group	Sample	Spiked (μM)	Detected (μM)	Recovery (%)	RSD (%), *n* =
1	*INH tablet (Local concentration of 3.12 μM)*	10	13.02	99.24	2.07
		15	18.92	104.4	3.67
		20	22.78	98.53	3.78
	Urine	10	9.68	96.80	2.98
		15	15.76	105.1	4.89
		20	12.17	95.85	2.11
	Serum	10	9.76	97.6	2.05
		15	15.32	102.1	3.86
		20	20.88	104.4	4.82
2	*INH tablet (Local concentration of 3.12 μM)*	10	12.79	97.48	2.46
		15	17.96	98.03	4.22
		20	23.42	101.3	3.71
	Urine	10	9.53	95.30	2.95
		15	14.43	96.20	3.08
		20	19.27	96.35	2.87
	Serum	10	9.95	99.50	4.12
		15	14.78	98.53	2.97
		20	19.22	96.10	3.96

References

[1] M. Segall, P.J. Lindan, M.a. Probert, C.J. Pickard, P.J. Hasnip, S. Clark, M. Payne, First-principles simulation: ideas, illustrations and the CASTEPcode, *J. Phys. Condens. Matter* 2002, **14**(11), 2717.

[2] J.P. Perdew, K. Burke, M. Ernzerhof, Generalized gradient approximation made simple, *Phys. Rev. Lett.* 1996, **77**(18), 3865.

[3] S. Grimme, Semiempirical GGA-type density functional constructed with a long-range dispersion correction, *J. Comput. Chem.* 2006, **27**(15), 1787-1799.

[4] D. Hamann, M. Schlüter, C. Chiang, Norm-conserving pseudopotentials, *Phys. Rev. Lett.* 1979, **43**(20), 1494.

[5] Y.-W. Mao, J. Zhang, R. Zhang, J.-Q. Li, A.-J. Wang, X.-C. Zhou, J.-J. Feng, N-doped carbon nanotubes supported Fe–Mn dual-single-atoms nanozyme with synergistically enhanced peroxidase activity for sensitive colorimetric detection of acetylcholinesterase and its inhibitor, *Anal. Chem.* 2023, **95**(22), 8640-8648.

[6] Z. Xi, K. Wei, Q. Wang, M.J. Kim, S. Sun, V. Fung, X. Xia, Nickel-platinum nanoparticles as peroxidase mimics with a record high catalytic efficiency, *J. Am. Chem. Soc.* 2021, **143**(7), 2660-2664.

[7] L. Gao, J. Zhuang, L. Nie, J. Zhang, Y. Zhang, N. Gu, T. Wang, J. Feng, D. Yang, S. Perrett, X. Yan, Intrinsic peroxidase-like activity of ferromagnetic nanoparticles, *Nat. Nanotechnol.* 2007, **2**(9), 577-583.
[8] Y. Fu, X. Zhao, J. Zhang, W. Li, DNA-based platinum nanozymes for peroxidase mimetics, *J. Phys. Chem. C* 2014, **118**(31), 18116-18125.
[9] J. Chen, Y. Yang, H. Kurban, Y. Xiao, L. Yang, W. Chen, S. He, Platinum coordination complex nanozymes with ligand-modulated peroxidase-like activity for sensitive biosensing, *ACS Appl. Nano Mater.* 2025, **8**(27), 13829-13837.
[10] X. Lai, Y. Han, J. Zhang, J. Zhang, W. Lin, Z. Liu, L. Wang, Peroxidase-like platinum clusters synthesized by ganoderma lucidum polysaccharide for sensitively colorimetric detection of dopamine, *Molecules* 2021, **26**(9), 2738.
[11] L. Chen, N. Wang, X. Wang, S. Ai, Protein-directed in situ synthesis of platinum nanoparticles with superior peroxidase-like activity, and their use for photometric determination of hydrogen peroxide, *Microchim. Acta* 2013, **180**(15), 1517-1522.
[12] L. Guan, Z. Wang, S. Li, P. Keoingthong, Z. Chen, CoPt graphitic nanozyme enabled naked-eye identification and colorimetric/fluorescent dual-mode detection of phenylenediamine isomers, *Chin. Chem. Lett.* 2026, **37**(2), 111323.
[13] R.P. Ojha, S. Pal, R. Prakash, Cu-Fe Prussian blue analog nanocube with intrinsic oxidase mimetic behaviour for the non-invasive colorimetric detection of isoniazid in human urine, *Microchem. J.* 2021, **171**, 106854.
[14] X. Wang, W. Ai, G. Chen, Y. Jin, J. Chen, F. Wang, T. Zhou, G. Zhang, Z. Zhang, Enhanced oxidase-like activity of Mo-MnO2 nanozymes for colorimetric sensing of isoniazid and ascorbic acid, *Colloid. Surfaces A* 2025, **708**, 136040.
[15] W. Zhu, Y. Cheng, C. Wang, X. Lu, Fabrication of a tubular CuO/NiO biomimetic nanozyme with synergistically promoted peroxidase-like performance for isoniazid sensing, *Inorg. Chem.* 2022, **61**(41), 16239-16247.
[16] J.-Q. Li, A.-J. Wang, P. Song, J.-J. Feng, Q. Zhou, T.Y. Cheang, Electronic structure modulation of ultrathin PtRuMoCoNi high-entropy alloy nanowires for boosting peroxidase-like activity and sensitive colorimetric determination of isoniazid and hydrazine, *Microchim. Acta* 2025, **192**(2), 82.
[17] Y. Dai, H. Zhang, Facile synthesis of copper carbonate analog with peroxidase-like activity for colorimetric detection of isoniazid, *Heliyon* 2024, **10**(15), e34962.
[18] X. Xie, Y. Zhao, Y. Fan, L. Jiang, W. Liu, X. Yang, Multifunctional Fe/Cu dual-single atom nanozymes with enhanced peroxidase activity for isoniazid detection and levofloxacin degradation, *Langmuir* 2024, **40**(24), 12671-12680.
[19] G. Li, Y. Yang, W. Chen, Z. Song, J. Shi, B. Wang, X. Pan, Z. Lin, Phenanthroline-functionalized donor–acceptor covalent organic frameworks as photo-responsive nanozymes for visual colorimetric detection of isoniazid, J. Mate. Chem. B 2024, **12**(18), 4502-4508.
[20] Z. Yuan, Y. Zhu, L. Xue, D. Ge, S. Xue, Y. Xie, W. Zhang, X. Chen, Hollow double shell Prussian blue analogue@ Au nanocubes with enhanced peroxidase-like activity for isoniazid detection in human serum, *Microchem. J.* 2025, **213**, 113799.
[21] S.-B. He, L. Yang, X.-L. Lin, L.-M. Chen, H.-P. Peng, H.-H. Deng, X.-H. Xia, W. Chen, Heparin-platinum nanozymes with enhanced oxidase-like activity for the colorimetric sensing of isoniazid, *Talanta* 2020, **211**, 120707.